

## DEVELOPMENT AND OPTIMIZATION OF SUPER SATURABLE SELF-NANO EMULSIFYING DRUG DELIVERY SYSTEM FOR DASATINIB BY DESIGN OF EXPERIMENT

C. RAJINIKANTH<sup>1\*</sup>, K. KATHIRESAN<sup>2</sup> 

<sup>1</sup>Department of Pharmacy, Faculty of Engineering and Technology, Annamalai University, Annamalainagar, Chidambaram 608303, Tamil Nadu, India. <sup>2</sup>Department of Pharmacy, FEAT, Annamalainagar, Chidambaram 608302, Tamil Nadu, India.

\*Corresponding author: C. Rajinikanth; \*Email: rajinichan@gmail.com

Received: 24 Jan 2024, Revised and Accepted: 20 Mar 2024

### ABSTRACT

**Objective:** In current research, Self-Nanoemulsifying Super Saturable Drug Delivery Systems S-SNEDDS was formulated to attain superior drug dissolution and stability.

**Methods:** Using saturated solubility, capryol ® 90, cremophor®-EL, and transcutool HP were used to make S-SNEDDS. Its composition was optimized using the ternary phase diagram. Using the central composite design of Response Surface Methodology, dasatinib-SNEDDS developed responses for droplet size (Y1), polydispersity index (Y2), and % drug released in 15 min (Y3). Various Precipitation Inhibitors were added to optimize SNEDDS (S3) to make S-SNEDDS and evaluate.

**Results:** The optimum formulation was S3, with a particle size of 128 nm and zeta potential of -21 mV. Methylcellulose was shown better supersaturation than other inhibitors. The optimized formulation (F3) was more stable than ordinary SNEDDS due to its more significant zeta potential (-25 mV) and lower particle size (128 nm). Dasatinib was shown to be amorphous in S-SNEDDS using Differential Scanning Calorimetry and X-ray Powder Diffraction. F3 had a higher 90 min release rate (>99%) than pure drug dispersion (26%) and SNEDDS formulation (95%).

**Conclusion:** The results concluded that S-SNEDDS formulation successfully enhanced the dissolution and stability of dasatinib.

**Keywords:** Dasatinib, Cancer, Central composite design, Super saturable self-nano emulsifying delivery system, Particle size

© 2024 The Authors. Published by Innovare Academic Sciences Pvt Ltd. This is an open access article under the CC BY license (<https://creativecommons.org/licenses/by/4.0/>)  
DOI: <https://dx.doi.org/10.22159/ijap.2024v16i3.50434> Journal homepage: <https://innovareacademics.in/journals/index.php/ijap>

### INTRODUCTION

The selective BCR-ABL kinase inhibitor dasatinib treats lung, prostate, and ovarian cancer [1]. It was approved by the FDA in 2006 as a small molecule to inhibit several tyrosine kinases. Acute lymphoblastic leukemia with chronic accelerated myeloid, lymphoid blast phase, and Philadelphia chromosome patients who have failed imatinib are treated with it as a second-line treatment [2]. Dasatinib was previously used only to treat adult patients, but new research has shown its potential in treating pediatric Chronic Myeloid leukemia (CML). Its pharmacokinetic properties, such as absorption and elimination time, were equivalent to those seen in adults, and it had the same safety and effectiveness profiles [3]. Dasatinib is a crystalline powder with pH-dependent solubility (18.4 mg/ml at pH 2.6 and 0.008 at pH 6.8). Dasatinib is a Biopharmaceutical Classification System (BCS) II medication with low solubility/high permeability [4]. It had 14%-34% oral bioavailability [5]. Dasatinib's side effects, including gastrointestinal problems, hemorrhage, and endothelial permeability, which can cause peripheral edema and pleural effusion, limit its clinical use [6]. Safe and effective dasatinib delivery vehicles could improve treatment efficacy and reduce systemic toxicity.

As a drug delivery vehicle, nanoparticles can improve bioavailability, specificity, tissue selectivity, and physiological action, increasing therapeutic efficacy [7, 8]. In the treatment of human cancers, nanoparticle-based drug delivery systems have several advantages over naked drugs, including improved drug solubility and stability, improved pharmacokinetics, Enhanced Permeability and Retention (EPR) effect-mediated tumor targeting, and the ability to engineer various functionalities [9, 10]. Nanocarriers could improve Dasatinib's water solubility, tumor-targeting efficacy, and side effects.

Polymeric micelles have been widely explored as dasatinib carriers, inhibiting tumor cell proliferation more than free dasatinib [11]. As carriers, albumin nanoparticles reduced dasatinib-induced endothelium hyperpermeability, enhancing anti-leukemia efficacy [12]. The regulated administration of dasatinib via layered polymer-coated carbon nanotubes improved its *in vitro* activity against U-87 glioblastoma cells

[13]. Gold nanoparticles coated with dasatinib enhanced therapeutic efficacy and reduced toxicity [14, 15]. Magnetic protein micelles improved dasatinib administration to triple-negative breast cancer cells. Recently, poly(cyclohexene phthalate) nanoparticles were found to transport dasatinib [16]. Although these nanocarriers are tiny and can increase cancer cell medication absorption and retention, they are unspecific and cannot control drug release.

Lipid-based formulations were selected to solve the aforementioned restrictions, and recently, Self-Nano-Emulsifying Drug Delivery Systems (SNEDDS) were created. Shown promising results in oral delivery of highly lipophilic medicines are preferred because of their simplicity of manufacture, practical improvement of oral bioavailability, and drug solubility. SNEDDS is an optically transparent anhydrous isotropic mixture comprising oil, surfactant, and co-surfactant. On coming in contact with gastrointestinal fluids, they disseminate as fine droplets of nanometric size. The SNEDDS may also cause drug precipitation in the gastrointestinal media, which lowers solubility and impairs drug bioavailability. The SNEDDS may also cause drug precipitation in the gastrointestinal media, which diminishes solubility and impairs drug bioavailability [17, 18]. To conquer these complexities and augment intestinal drug absorption, the super saturable-SNEDDS (S-SNEDDS) was proposed. S-SNEDDS represents a novel technique comprising a water-soluble precipitation inhibitor proposed to produce and preserve a meta-stable supersaturation state by avoiding or diminishing drug precipitation [19, 20].

The Response Surface Method (RSM) uses statistical approaches to improve or optimize manufacturing [21]. Thus, statistical Design of Experiment (DoE) has grown more popular in the formulation in recent years. With proportionally fewer experimental runs, DoE accurately estimates factor effects and interactions and optimizes by grid-searching the factor space. DOE requires fewer experimental runs and shows (any) synergism or interaction between components, resulting in a robust formulation with economic time, money, and development benefits [22]. Most RSM experiments use Central Composite Designs (CCD). CCDs are factorial or fractional factorial designs with center points and axial points (star points) to estimate

curvature [23]. CCD arrays have circumscribed factor levels on the edges, center, and side. Central Composites fit entire quadratic models. These designs can contain data from a well-planned factorial experiment, making them famous for sequential experimentation [24]. The current research aims to develop S-SNEDDS of dasatinib by employing CCD to assess the effects of formulation variables on responses.

## MATERIALS AND METHODS

### Materials

Dr Reddy's Laboratories Limited (Hyderabad, India) gave dasatinib as gift sample. Merck Life Science Private Limited (Hyderabad, India) supplied Capryol® 90, Caprylic and capric acid triglycerides (LabrafacLipophile WL 1349 and Captex® 300), Mainsine®-35, Lauroglycol® 90, and Peceol®. SD Fine Chemicals Limited (Ahmedabad, India) sold Cremophor®-EL, Tween® 80, Tween® 20, Span® 80, Span® 20, Cremophor® RH40, Labrasol®, Propylene glycol, Ethanol, PEG 400, PEG 600, and Transcutol Dialysis membrane (DM-70; MWCO 10000) was purchased from Hi-media (Mumbai, India). All other chemicals were analyzed and utilized without further purification.

### Methods

#### SNEDDS formulation

#### Selection of formulation excipients

To monitor suitable oil, surfactant and co-surfactant, the solubility saturation of dasatinib in several vehicles was analyzed as per the preferred method [25]. A precisely calculated quantity of supernatants was suitably diluted using carbinol, and the amount of dasatinib was determined with a UV spectrophotometer (Shimadzu-1200) at 330 nm.

#### Establishment of ternary phase diagram

The self-nanoemulsifying region evaluated from ternary diagrams (using XLSTAT add-on statistical software) comprises the three excipients as the triangle's apex [26]. The formulation excipients were mixed and vortexed for 60 sec to assist homogenization. The

effectiveness of nanoemulsion development was evaluated by mixing 100 mg with 25 ml of water trailed by moderate physical agitation. The formulations were evaluated for easiness of emulsification and visual appearance.

#### Compatibility study of drug-excipient

The Fourier-Transform Infrared Spectroscopy (FTIR) was utilized to record the drug's spectra and physical mixture (1:1) by using FTIR Spectrophotometer (Shimadzu FTIR 8400S, Japan) scanned between 4000 to 400 cm<sup>-1</sup>. The Differential Scanning Calorimetry (DSC) was recorded using Perkin Elmer DSC/7 DSC equipment. The SEM study was conducted using a Hitachi S-3000 N with a hastening voltage of 10 Kv and a magnification of 5000X.

#### Design of experiment-CCD

A 3<sup>2</sup>CCD was used to investigate and optimize various effects of formulation excipients on SNEDDS (table 1). Twenty model experiments were conducted using Stat-Ease Design Expert® software V8.0.1, which provides a CCD model. According to the conditions specified in table 2 and the results tabulated. As illustrated in Equation 1, Individual response parameters were evaluated using quadratic models with repeated linear regression analysis for each response parameter.

$$Y = \beta_0 + \beta_1 X_1 + \beta_2 X_2 + \beta_3 X_1 X_2 + \beta_4 X_1^2 + \beta_5 X_2^2 + \beta_6 X_1 X_2^2 + \beta_7 X_1^2 X_2 \quad (1)$$

Y-The magnitude of the measured response

$\beta_0$ -intercept

$\beta_1$ - $\beta_7$ -regression coefficients

$X_1, X_2$ -main effects

$X_1, X_2$ -interaction among  $X_1, X_2$

$X_1^2$  and  $X_2^2$ -quadratic terms

The effects of A, B, and C on Y1 and Y2 were evaluated from the plot [27]. Derringer's functionality of desirability was used to calculate the optimal SNEDDS configuration.

Table 1: The CCD variables

Independent-variables			Stages			
Variables	Name	Unit	Low(-1)	High(+1)	- $\sigma$	+ $\sigma$
A	Quantity of Capryol® 90	Mg	25	40	19.88	45.11
B	Amount of Cremophor®-EL	mg	30	60	19.77	70.23
C	Amount of Transcutol® HP	mg	20	35	14.88	40.11
Dependent variable			Goal			
Y <sub>1</sub>	DLS	Nm	Minimum			
Y <sub>2</sub>	PDI		Minimum			
Y <sub>3</sub>	DR	%	Maximum			

PDI-Polydispersity index, DR-Drug release in 15 min, DLS-Droplet size

Table 2: CCD with observed responses

Run	Capryol® 90 (mg)	Cremophor®-EL (mg)	Transcutol® HP (mg)	DLS (nm)	PDI	DR
1	25	60	35	190.24	0.241	68.83
2	40	30	20	208.73	0.267	64.67
3	32.5	19.77	27.5	166.76	0.195	71.26
4	45.11	45	27.5	229.56	0.243	64.16
5	32.5	45	27.5	194.87	0.219	70.75
6	32.5	45	27.5	195.76	0.218	71.06
7	25	60	20	166.93	0.196	72.17
8	32.5	45	27.5	193.47	0.222	71.12
9	40	60	35	254.55	0.328	65.19
10	40	30	35	192.32	0.208	70.96
11	32.5	45	40.11	200.43	0.282	70.12
12	32.5	45	27.5	195.13	0.198	69.72
13	32.5	45	14.88	192.93	0.283	69.56
14	25	30	35	131.76	0.132	72.86
15	32.5	70.22	27.5	164.73	0.236	70.89
16	19.88	45	27.5	188.82	0.162	67.94
17	32.5	45	27.5	195.86	0.219	69.45
18	25	30	20	224.43	0.242	67.26
19	40	60	20	147.12	0.214	70.16
20	32.5	45	27.5	197.67	0.212	70.12

### Selection of precipitation inhibitor

Various S-SNEDDS were formulated by mixing various precipitation inhibitors with the optimized SNEDDS formulation. 1000 mg of optimized dasatinib SNEDDS and precipitation inhibitors were mixed with 100 ml of Simulated Gastric Fluid (SGF) medium at 37 °C and 100 rotations per minute. 1 ml of this solution was withdrawn at predetermined intervals between 5 and 240 min, followed by centrifugation for 3 min. The supernatant was mixed with carbinol, and the amount of dasatinib was evaluated spectrophotometrically.

### Preparation of dasatinib-loaded SNEDDS and S-SNEDDS formulation

Drug-loaded SNEDDS was formulated by dissolving dasatinib in oil, surfactant and co-surfactant. To accomplish complete drug solubility, the components were combined by swirling and vortexing at 37 °C. S-SNEDDS formulation is carried out by adding various amounts of selected precipitation inhibitor to optimized SNEDDS formulation [28].

### Estimation of droplet size and zeta potential

In collaboration with the particle sizing software MAS OPTION, Mastersizer 2000 (Malvern Instruments Ltd, UK) was used to measure the DLS. The zeta potential was analyzed using an additional electrode fitted to the above equipment.

### The Scanning Electron Microscope (SEM) analysis

The external surface and cross-section of the drug and SNEDDS were evaluated using an S4100, Hitachi, Japan SEM instrument at 15 keV accelerating voltage. For contrast enhancement, one drop of diluted emulsion was put on a film-coated copper grid and stained with one drop of a 2 percent (w/v) aqueous phosphotungstic acid solution before drying. SEM was used to evaluate the samples at a magnification of 72000.

### Thermodynamic stability study

This was tested after six cycles of chilling (4 °C) and heating (40 °C), followed by 48 h of freeze-thaw cycles (-21 °C and 25 °C). The stable

formulation was evaluated for centrifugation at 3500 rotations per minute for 30 min and examined for phase separation [29].

### Physicochemical characterization

The formulated SNEDDS and S-SNEDDS were subjected to FTIR, DSC, powdered XRD, and SEM analysis.

### In vitro dissolution study

The experiments used a USP type II device (Electrolab, TD L8, India) at 50 rpm. The samples containing 10 mg of dasatinib were mixed with 0.9 L of medium (pH 6.8 buffer solution) comprised of 0.5% Tween 80 at 37 °C. At present time slots, about 5 ml samples were removed and replaced with a proportionate new medium. The contents were filtered, diluted duly, and evaluated for drug content. All measurements were taken in triplicate [30].

### Kinetic analysis

The *in vitro* dissolution data were entered into several release kinetic models to evaluate release order and release mechanism [31].

### Accelerated stability study

The formulation's stability was assessed using ICH guidelines Q1A (R2) by storing samples in a stability chamber at 40 °C and 75 percent relative humidity for three months and analyzing the results [32].

## RESULTS AND DISCUSSION

### Solubility study

Drug solubility is important while formulating SNEDDS to avoid precipitation. SNEDDS-soluble, poorly soluble medicines that precipitate when diluted by stomach juices or aqueous dispersion. The solubility results displayed the highest drug solubility in capryol 90, cremophor®-EL, and transcutool® HP, chosen as excipients (fig. 1). SNEDDS components should solubilize the most medication and have a bigger self-emulsification zone in the ternary phase diagram [19].

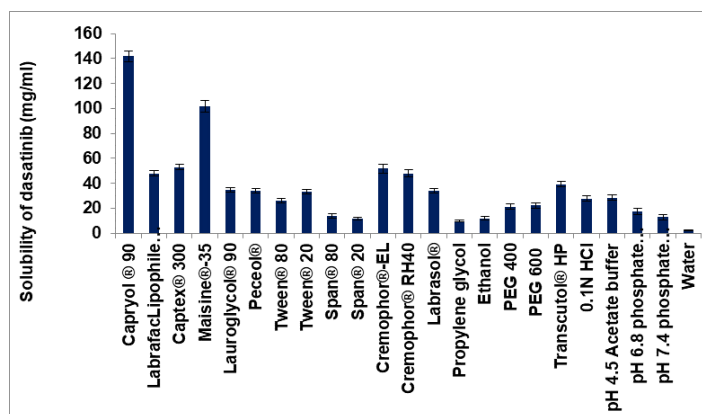


Fig. 1: Solubility of dasatinib in various vehicles (All determinations were performed in triplicate and values were expressed as mean±SD, as error bart, n=3)

### Selection of oil, surfactant, co-surfactant

The oil phase is crucial to the formulation of SNEDDS because its physicochemical properties-molecular volume, polarity, and viscosity-determine the spontaneity of the nanoemulsification process, droplet size, drug solubility, and biological fate [20]. Due to its impact on formulation-loading capacity and medication absorption, the oil with the greatest solubilization ability is typically chosen [22]. The chosen oil should also produce nanoemulsions with tiny droplets [21]. The choice of oily phase is frequently a compromise between solubilizing the medication and forming a nanoemulsion with desirable properties.

The second mandatory component in SNEDDSs is surfactants, and their choice is crucial for formulation. Surfactant parameters like HLB (in oil), cloud point, viscosity, and affinity for the oily phase affect nanoemulsion droplet size, self-emulsification area, and process [19]. To facilitate nanoemulsion dispersion, the surfactant must drop interfacial tension to a very low value. To achieve the desired interfacial curvature, the surfactant should be lipophilic [24].

One surfactant seldom provides low interfacial tension; a co-surfactant is generally needed [18]. They work synergistically with surfactants to improve medication solubility and dispersibility in the oil phase, stabilizing and homogenizing nanoemulsions. Co-

surfactants improve interfacial fluidity, reducing surfactant local irritancy and formulation dosage variability. Due to their polarity, co-surfactants should be used sparingly to enhance medication solubilization. Co-surfactants move to the water phase after aqueous dispersion, causing drug precipitation [21]. Hence, this investigation chose SNEDDS oil based on its ability to solubilize the most medication. The emulsification potential of each surfactant was assessed by the amount of oil it emulsified. Due to their polarity, co-surfactants should be used sparingly to improve medication solubilization. Co-surfactants move to the water phase after aqueous dispersion, causing drug precipitation [32].

### Ternary phase diagram

The phase diagram constructed for cremophor®-EL/transcutol® HP systems indicated an increase in nano-emulsion area with an

increase in cremophor®-EL to transcutol® HP ratio; this was clarified by surfactant adsorption at the emulsion interface rises; lowering surface tension and droplet size. Each component's range was optimized as per the diagram.  $20\% \leq \text{Capryol}90 \leq 40\%$ ,  $30\% \leq \text{Cremophor}^{\circledR}\text{-EL} \leq 60\%$ ,  $20\% \leq \text{Transcutol}^{\circledR}\text{ HP} \leq 30\%$ .

An emulsification region was found in a pseudo-ternary phase diagram to improve the formulations (fig. 2). Gentle agitation creates a transparent, translucent fine oil in water emulsion [17]. Shaded areas indicate formulations with the highest potential of creating nano-emulsions of  $>200$  nm droplet size, while formulations with greater globule size have low emulsion formation capabilities. Nano-emulsification occurs when aqueous dispersion produces homogeneous, transparent systems. Due to limited water solubility, certain drug molecules may orient at nano-emulsion interfaces [19].

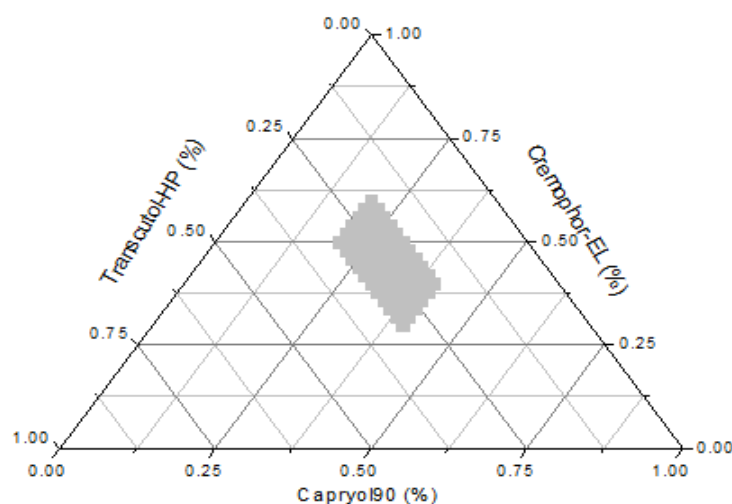


Fig. 2: Ternary phase diagram of dasatinib-loaded SNEDDS

### Drug and excipients compatibility study

To establish the identification of the drug and excipients and the interaction of the drug with the excipients, FTIR absorption spectra of pure drug, all chosen excipients utilized, and the physical combination of drug and excipients were collected. The major characteristic peaks

at 3408.33, 3205.80, 2949.26, 2821.95, 1612.54, 1577.82, 1502.6, 1444.73, 1390.72, 1290.42, 1215.19, 1193.98, 1003.02, 862.21, 813.99, 773.48 and 590.24  $\text{cm}^{-1}$  verifying dasatinib purity as per the established standards. The principal peaks of dasatinib appeared at equivalent wave numbers, indicating the lack of any physical interactions of the drug with the selected excipients (fig. 3).

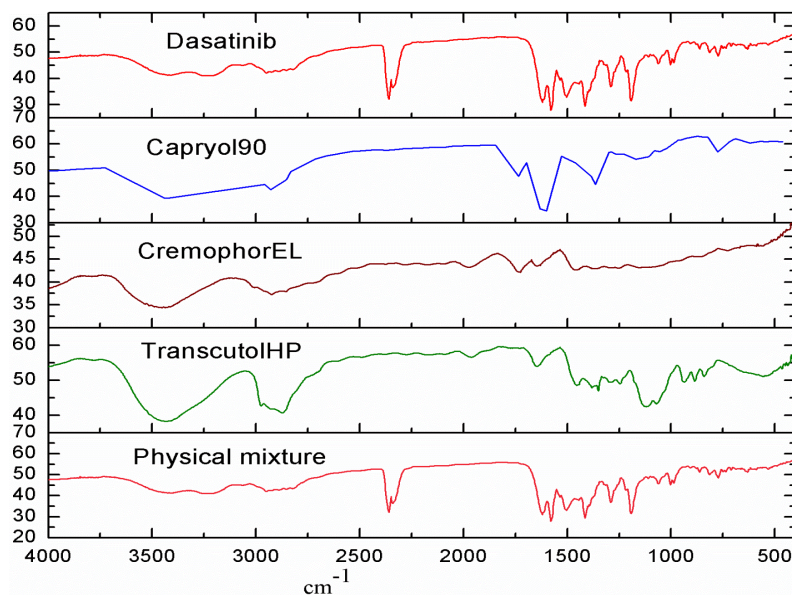


Fig. 3: FTIR spectrum of dasatinib, excipients, and physical mixture

Dasatinib's DSC thermogram (fig. 4) revealed a prominent endothermic peak at 291 °C, matching its melting point. DSC of Capryol® 90 revealed an endothermic peak at 107.1 °C. The DSC curve of cremophor®-EL has shown an endothermic peak at 360.49 °C. The DSC curve of transistor HP has shown an endothermic peak

at 116.92 °C. The thermogram of the physical mixture displayed two endothermic peaks of transistor HP and dasatinib. A DSC thermogram of the material mixture illustrated the drug's clear, distinct endothermic peak, which indicates the nonexistence of any physical interactions with the selected excipients.

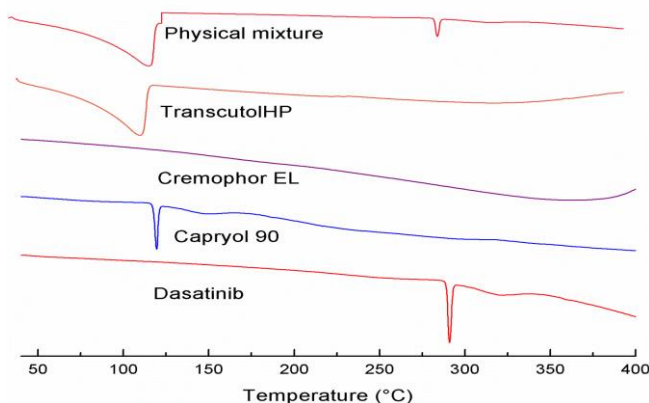


Fig. 4: DSC thermogram of dasatinib, excipients, and physical mixture

**Design of experiments**

About 20 trials were carried out based on the experimental runs obtained from a CCD. The range of droplet size (Y<sub>1</sub>) was 131.76-254.55 nm, the polydispersity index (Y<sub>2</sub>) was 0.132-0.328, as well as the percent drug release range in 15 min (Y<sub>3</sub>), was in the

range 64.16-72.86% (fig. 5). The obtained responses were substituted into the quadratic model, and results showed a non-significant lack of fit (p>0.1), confirming the sufficiency of model fit. Multiple regression analysis for the 2nd-order quadratic model (R<sup>2</sup>) signifies the measurement of variation in the region of the mean [34].

**Design Summary**

<b>Study Type</b>	Response Surface	<b>Runs</b>	20
<b>Design Type</b>	Central Composite	<b>Blocks</b>	No Blocks
<b>Design Model</b>	Quadratic	<b>Build Time (ms)</b>	3.47

Factor	Name	Units	Type	Subtype	Minimum	Maximum	-1 Actual	+1 Actual	Mean	Std. Dev
A	Amount of capryol90	mg	Numeric	Continuous	19.89	45.11	25.00	40.00	32.50	6.20
B	Amount of cremophor EL	mg	Numeric	Continuous	19.77	70.23	30.00	60.00	45.00	12.40
C	Amount of transcutol HP	mg	Numeric	Continuous	14.89	40.11	20.00	35.00	27.50	6.20

Response	Name	Units	Obs	Analysis	Minimum	Maximum	Mean	Std. Dev.	Ratio	Trans	Model
Y <sub>1</sub>	Droplet size	nm	20	Polynomial	131.76	254.55	191.604	27.5973	1.93192	None	RQuadratic
Y <sub>2</sub>	PDI		20	Polynomial	0.132	0.328	0.22585	0.0433824	2.48485	None	RQuadratic
Y <sub>3</sub>	Drug release after 15min	%	20	Polynomial	64.16	72.86	69.4125	2.42386	1.1356	None	RQuadratic

Fig. 5: Summary of the CCD

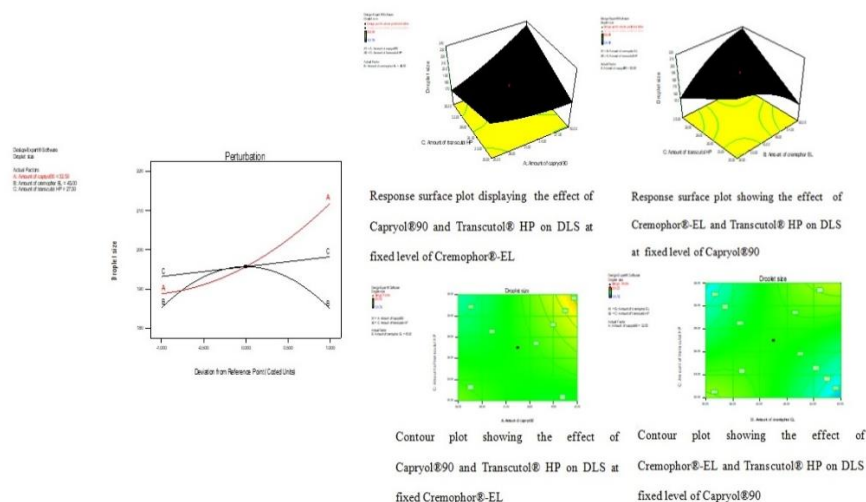


Fig. 6: Perturbation, 3D response surface, and counterplots display the influence of formulation parameters on DLS

The mathematical droplet size (Y1) model had an F-value of 954.74, indicating significance. A significant "Model F-value" owing to noise is 0.01% likely. Model terms are significant if "Prob>F" is less than 0.0500. A, C, AC, BC, A<sup>2</sup>, and B<sup>2</sup> significantly affect droplet size. Model terms above 0.1000 are insignificant—the significant model terms with P values < 0.0500. "Lack of Fit F-value" of 1.23 indicates it is negligible compared to pure error. A "Lack of Fit F-value" this large is 42.59% likely attributable to noise. A has a more significant influence than C, according to the equation. The droplet size factorial equation correlated well (0.9972). Plots of the perturbation, contour, and 3D response surface revealed independent factors' primary and interacting impacts on droplet size. The perturbation plot demonstrates what kind of effects A, B, and C have on droplet size (Y1). This graph shows that A has the highest influence on Y1, followed by C, which has little impact. Fig. 6 shows the contour plots and interactions between A and C on droplet size at a fixed level of B and A. At low A levels, Y1 dropped from 224.43 to 131.76 nm. At high A levels, Y1 dropped from 254.55 to 147.12 nm. At low B levels, Y1 dropped from 224.43 to 131.76 nm. At high B levels, it dropped from 254.55 to 147.12 nm. Y1 dropped from 224.43 to 147.12 nm at low C. At high C levels, Y1 dropped from 254.55 to 131.76 nm. Many SNEDDS articles describe an increase in droplet size with an increase in oil (A) and co-surfactants (C) or vice versa. High co-surfactant concentrations and oil amounts may form a thick layer on oil droplets, stabilizing them.

Table 2 shows that the prepared SNEDDS had a polydispersity index of 0.132–0.328. The quadratic model showed that Capryol® 90 and Cremophor®-EL affect the polydispersity index. Table 4 shows that theoretical (predicted) and observed values were close. An F-value of 95.33 indicates that the polydispersity index (Y2) mathematical model is noteworthy. A significant "Model F-value" owing to noise is 0.01% likely. Model terms are essential if "Prob>F" is less than 0.0500. A, B, AC, BC, A<sup>2</sup>, and C<sup>2</sup> are essential model terms. Model terms with "Prob>F" larger than 0.1000 are insignificant. Lack of Fit is insignificant relative to a pure error with a "Lack of Fit F-value" of 0.45. A "Lack of Fit F-value" this large is 83.61% likely attributable to noise. Non-significant misfit is good—we want the model to fit. The equation shows that A is more significant than B. The polydispersity index factorial equation found an excellent correlation (0.9823). The perturbation, contour, and 3D response surface plots revealed independent factors' primary and interacting effects on the polydispersity index. The perturbation plot reveals B and C on critical effects on Y2 polydispersity. B has the most significant impact on Y2, followed by C with minimal impact. Fig. 7 shows the PDI interconnection between A and C at a constant B and C level at a specified A level and their contour plots. At low A levels, Y2 dropped from 0.242 to 0.132. Similarly, high A levels dropped Y2 from 0.328 to 0.208. At low B, Y2 dropped from 0.267 to 0.132. At high B levels, Y2 dropped from 0.328 to 0.196. Y2 dropped from 0.267 to 0.196 at low C. At high C levels, Y2 dropped from 0.328 to 0.132.

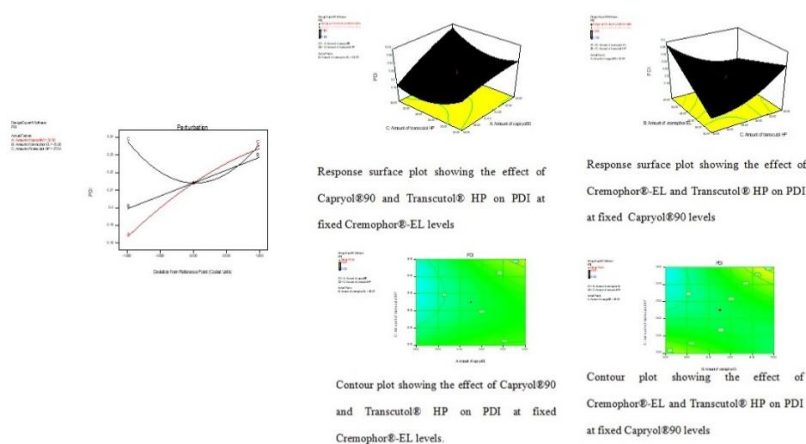


Fig. 7: Perturbation, 3D response surface, and counterplots display the influence of formulation excipients on PDI

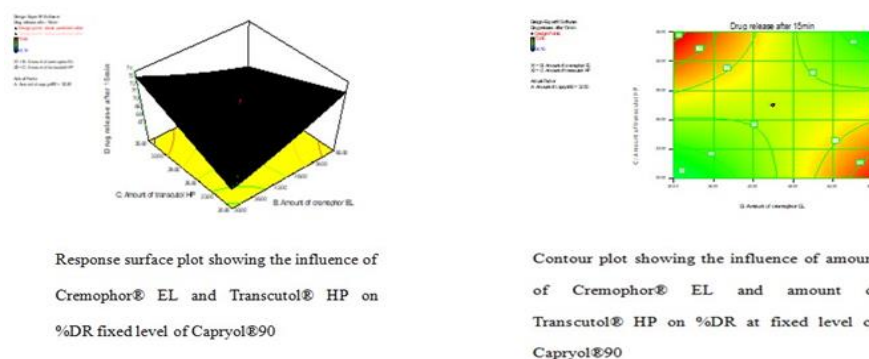


Fig. 8: 3D response surface and counterplot display the influence of formulation excipients on percent drug release

The SNEDDS formulations' percent drug release in 15 min varied from 64.16 to 72.86 percent (table 2). The model revealed that the level of capryol®90 has a significant negative influence on the % drug release after 15 min.

#### Optimization by desirability function

The responses were converted into the desirability scale, with Y<sub>1</sub> and Y<sub>2</sub> being minimum and Y<sub>3</sub> being maximum. The maximum function value was obtained at A: 25, B: 30, and C: 35 (w/w). Three

batches of SNEDDS at optimal conditions were planned to validate the adequacy of prediction, and answers were assessed (table 3). The model was considered valid since there was a close correlation between predicted and observed values.

#### Evaluation of SNEDDS

Droplet size, polydispersity index and zeta potential of the diluted dasatinib-SNEDDS were measured. Droplet size is crucial for SNEDDS evaluation. Smaller droplets increase medication absorption surface

area. A smaller droplet size may also speed release [19]. The stability of colloidal dispersions may affect zeta potential, where a kinetically stable emulsion system requires adequate emulsion droplet repulsion [20]. The PDI of optimized SNEDDS was measured post-with 100

times dilution in distilled water. The DLS and PDI of optimized SNEDDS were 128-131 nm and 0.138-0.146. The ZP of optimized SNEDDS ranged between -21 and -23 mV. The formulation S3 with the least particle size was considered for formulation into S-SNEDDS.

Table 3: Regression equations

Response	Linear regression equation
Y <sub>1</sub>	195.71+11.56A+2.51 C+20.05 AC+29.98 BC+4.67 A <sup>2</sup> -10.69 B <sup>2</sup>
Y <sub>2</sub>	0.21+0.025 A+0.015 B+0.015 AC+0.041 BC+0.023 C <sup>2</sup>
Y <sub>3</sub>	70.23-1.21 A-2.53 BC-1.49 A <sup>2</sup>

Table 4: Optimized values obtained by the constraints applied on Y<sub>1</sub>, Y<sub>2</sub>, and Y<sub>3</sub>

Independent variable	Nominal values	Predicted			Observed				
		Droplet size (Y <sub>1</sub> ) (nm)	Poly-dispersity index (Y <sub>2</sub> )	% drug release in 15 min (Y <sub>3</sub> )	Batch	Droplet size (Y <sub>1</sub> ) (nm)	Poly-dispersity index (Y <sub>2</sub> )	% Drug release in 15 min (Y <sub>3</sub> )	ZP (mV)
A	25 mg				S1	131.13	0.138	72.78	-22.3±1.12
B	30 mg	130.75	0.134	73.09	S2	129.84	0.146	71.96	-23.7±2.13
C	35 mg				S3	128.96	0.142	72.06	-21.8±1.98

### Screening of precipitation inhibitor

S-SNEDDS are designed to surrender to a supersaturated state, so it's necessary to measure the drug concentration and degree of supersaturation over time. To create S-SNEDDS, polymers such as HPMC K4M, PVP K30, Poloxamer 407, and Eudragit L100 were added to the optimized SNEDDS (S3) [35]. Based on the design of the experiment, formulation S3 with minimum DLS and optimal ZP was chosen for formulation into S-SNEDDS. The precipitation profile indicated that the S-SNEDDS displayed superior reticence

of drug precipitation compared to SNEDDS within 240 min. The dasatinib concentration in the test medium was calculated to be 1000 µg/ml based on the 100 dilution factor (i.e., 10 mg dasatinib in 100 ml medium). At t = 15 min, dasatinib in SNEDDS reduced to 312 µg/ml and swiftly to 241 µg/ml post 30 min owing to drug precipitation. In disparity, the S-SNEDDS formulation displayed a constantly superior dasatinib concentration-time profile than that of SNEDDS. The results indicate that the HPMC could more effectively preserve the drug in a supersaturation state than other inhibitors. (fig. 9).

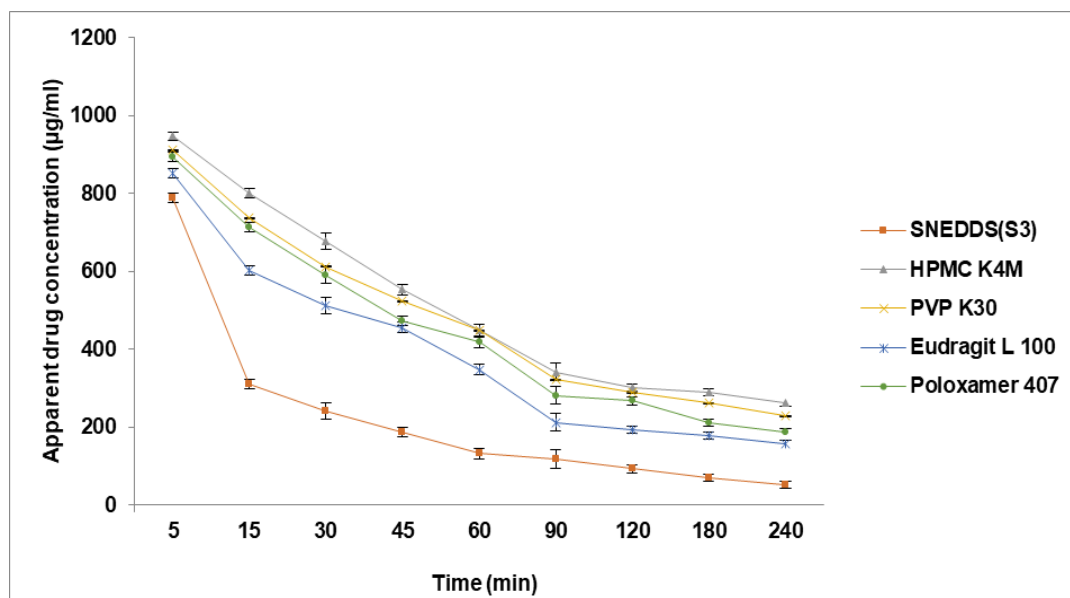


Fig. 9: *In vitro* mean apparent dasatinib concentration-time profiles observed from various polymer PIs, (All determinations were performed in triplicate and values were expressed as mean±SD, as error bars, n=3)

To establish the effect of HPMC K4M on supersaturation states, a sequence of dasatinib S-SNEDDS was prepared using varying amounts of HPMC. The results indicated that the precipitation inhibition outcome was improved with an increase in HPMC K4M concentration. No significant variation in the effectiveness of HPMC K4M within 2.0% or 5.0%. All the formulations displayed shorter emulsification time < 1 min, indicating higher self-emulsification effectiveness. Hence, 2% HPMC K4M (F3) was chosen for further studies.

### The droplet size and zeta potential of S-SNEDDS

The droplet size of S-SNEDDS (F1-F4) ranged from 128-131 nm with poly dispersity index 0.122-0.132, which is somewhat less than SNEDDS (131-254 nm) due to addition of HPMC that produced a physical barrier that surrounds the oil droplets thus preventing aggregation to obtain smaller size nanoemulsion (table 5).

Table 5: The DLS, PDI, and ZP of S-SNEDDS formulations

Sample	Droplet size (nm)	Polydispersity index	Zeta potential (mV)
F1	129.34±1.54	0.132±0.005	-24.12±2.1
F2	128.23±1.23	0.137±0.005	-25.46±1.8
F3	128.16±0.96	0.122±0.005	-23.45±1.4
F4	131.13±2.11	0.128±0.005	-21.87±1.8

(All measurements were performed in triplicate, and results were reported as mean SD (n=3))

#### Thermodynamic stability

The S-SNEDDS formulation (F3) generated a translucent emulsion that was evaluated at various temperatures and stress levels after dispersion in water. The chosen formulation passed the thermodynamic stability test with no phase separation or precipitation over alternate Temperature cycles (4 and 40 degrees Celsius), freeze-thaw cycles (-21 and +25 degrees Celsius), and

centrifugation at 3500 all demonstrated satisfactory formulation stability.

#### Physicochemical characterization of dasatinib S-SNEDDS

The interaction between dasatinib and precipitation inhibitor was evaluated by FT-IR spectroscopy. The peak at 2949.26  $\text{cm}^{-1}$  in dasatinib (fig. 10) shifted to 3075.35  $\text{cm}^{-1}$  in S-SNEDDS.

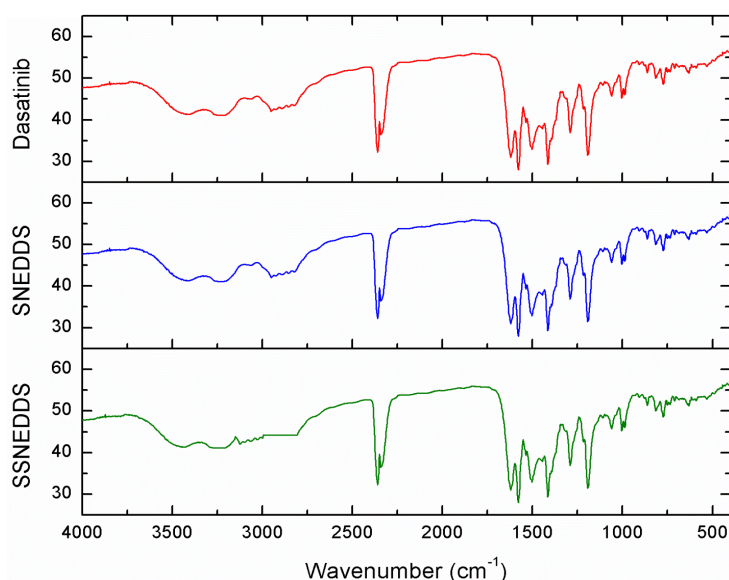


Fig. 10: FTIR of pure dasatinib, dasatinib SNEDDS and dasatinib S-SNEDDS, in the XRPD pattern of S-SNEDDS, the peaks of dasatinib were faint or vanished, demonstrating a decline in the crystalline nature of dasatinib (fig. 11).

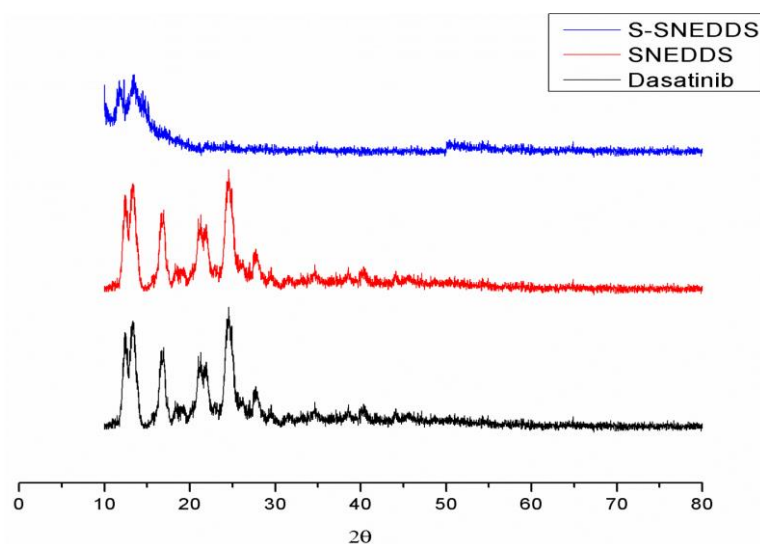


Fig. 11: XRD spectra of pure dasatinib, dasatinib SNEDDS, and S-SNEDDS

Dasatinib and S-SNEDDS displayed sharp endotherm peaks at 291 °C and 302.4 °C, corresponding to the melting point of the drug. The S-

SNEDDS displayed no specific peak between 40 °C and 400 °C, confirming the amorphous nature of the drug (fig. 12).

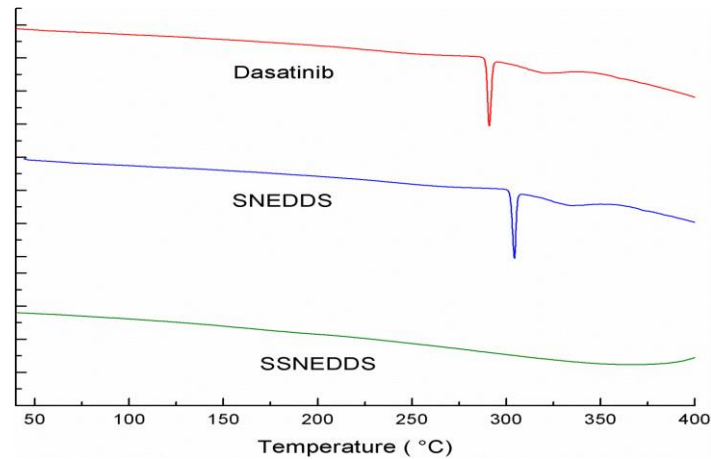


Fig. 12: DSC thermograms of dasatinib pure drug, dasatinib SNEDDS and S-SNEDDS

### SEM analysis

The SEM studies confirmed that the SNEDDS and S-SNEDDS are in regular spherical shape and size (The samples were analyzed using SEM at 72000× magnification; fig. 13).

### In vitro dissolution results

The S-SNEDDS dissolution profile was superior ( $31.28 \pm 1.4\%$  within 5 min) to that of pure drug dispersion and SNEDDS (fig. 14). Quick drug dissolution of S-SNEDDS owing to lower surface free energy that facilitates immediate emulsification by establishing interface among dissolution medium and oil. The

enhanced dissolution of 99% observed in 90 min may be attributable to the fact that Dasatinib was transformed from a low-solubility crystalline to an amorphous state, resulting in an enhanced nanosized globule surface area.

### Release kinetics

The results show that the regression coefficient value is nearing 1 in the case of first-order kinetics for optimized formulation with  $n = 52.17$  from the Korsmeyer-Peppas plots confirming. The medication was released via the super case II transport mechanism. The drug release kinetics data is shown in table 6.

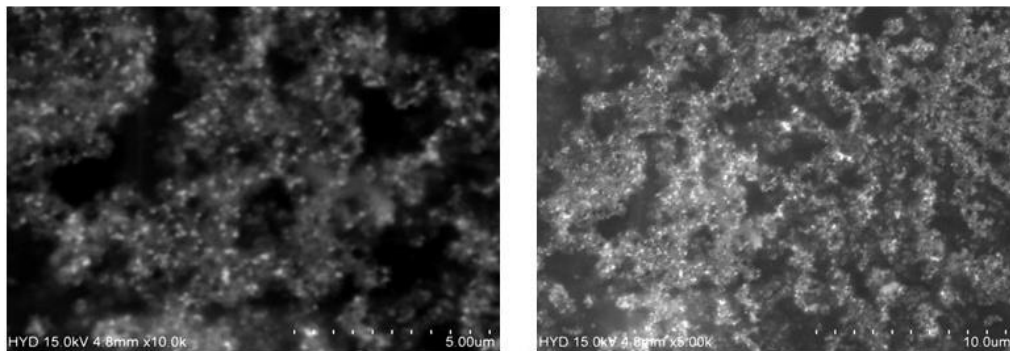


Fig. 13: SEM images of dasatinib-loaded SNEDDS (S3) and S-SNEDDS (F3) formulation at 72000× magnification

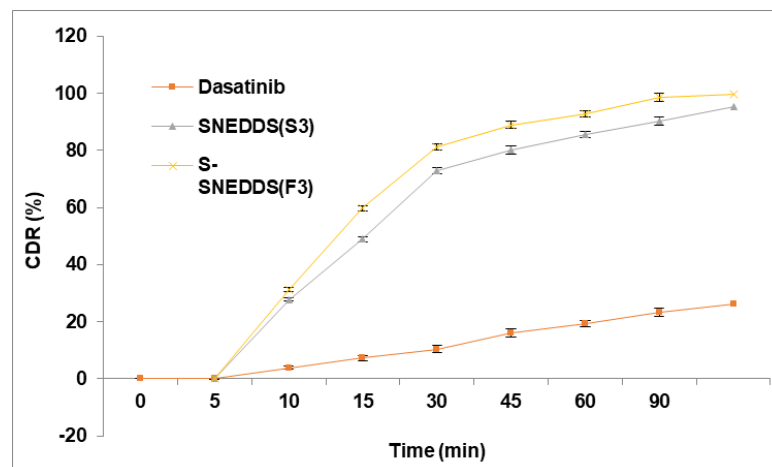


Fig. 14: Dissolution profile of dasatinib from SNEDDS and S-SNEDDS formulation (All measurements were performed in triplicate, and results were reported as mean SD as error bars,  $n=3$ )

Table 6: Release kinetics of optimized formulation of dasatinib SNEDDS

Formulation code	Zero-order		First order		Higuchi		Korsmeyer-peppas	
	R <sup>2</sup>	n	R <sup>2</sup>	n	R <sup>2</sup>	n	R <sup>2</sup>	N
F2	0.5218	0.890	0.9762	-0.0273	0.8053	10.623	0.863	52.17

Table 7: Droplet size, zeta potential, and polydispersity of dasatinib S-SNEDDS formulation after 90 d of storage

Temperature (°C)	Droplet size (nm)		Zeta potential		Polydispersity index	
	0 mo	3 mo	0 mo	3 mo	0 mo	3 mo
4±1 °C	128.96±0.96	130.12±2.04	-23.45±1.4	-21.76±1.6	0.122±0.005	0.132±0.005
25±2 °C	128.96±0.96	129.56±1.23	-23.45±1.4	-23.12±2.1	0.122±0.005	0.141±0.005

(All measurements were performed in triplicate, and results were reported as mean SD n=3)

### Stability study

Table 7 displayed no considerable divergence ( $p < 0.05$ ) in droplet size, zeta potential, and poly dispersity of optimized formulation maintained at ambient and refrigerated temperatures.

### CONCLUSION

The dasatinib-SNEDDS were successfully formulated by capryol@ 90, cremophor@-EL, and transcuto HP, displaying a faster self-emulsifying time, optimal DLS, and ZP. Based on the experimental runs, twenty experiments were carried out obtained from a CCD, and analyzed by Design-Expert software. The optimized formulation (S3) chosen from ternary phase diagram and CCD composed of capryol@ 90: 25%, cremophor@-EL30% and transcuto HP: 35% (w/w) was further incorporated with HPMC to convert to supersaturable SNEDDS which displayed rapidly *in vitro* drug dissolution of over 99% in 90 min which is superior to that of SNEDDS (S3) release of 95% and pure drug dissolution of 26%. The increased surface area of nanosized globules and the transition of dasatinib from crystalline to amorphous state may be linked to better dissolution. The stable supersaturate formulation had the advantages of superior emulsifier ability and provided constructive oral solid dosage form for poorly water-soluble drugs.

### ACKNOWLEDGEMENT

The authors express their gratitude to the Management and Department of Pharmacy at Annamalai University, located in Annamalai Nagar, Chidambaram, Tamil Nadu, India, for their provision of research facilities.

### FUNDING

Nil

### AUTHORS CONTRIBUTIONS

CR completed the research work, execution, and writing. KK did the work plan, review, and corrections. All authors agree with the submission and publication. All authors have read and agreed to the published version of the manuscript.

### CONFLICT OF INTERESTS

The authors declare that they have no competing interests in this research.

### REFERENCES

- Ceppi P, Papotti M, Monica V, Lo Lo Iacono M, Saviozzi S, Pautasso M. Effects of SRC kinase inhibition induced by dasatinib in non-small cell lung cancer cell lines treated with cisplatin. *Mol Cancer Ther.* 2009;8(11):3066-74. doi: 10.1158/1535-7163.MCT-09-0151, PMID 19861409.
- Agrawal M, Garg RJ, Cortes J, Quintas Cardama A. Tyrosine kinase inhibitors: the first decade. *Curr Hematol Malig Rep.* 2010;5(2):70-80. doi: 10.1007/s11899-010-0045-y, PMID 20425399.
- Gore L, Kearns PR, de Martino ML, Lee CADS, De Souza CA, Bertrand Y. Dasatinib in pediatric patients with chronic myeloid leukemia in chronic phase: results from a phase II trial. *J Clin*

- Oncol.* 2018;36(13):1330-8. doi: 10.1200/JCO.2017.75.9597, PMID 29498925.
- Wang C, Wang M, Chen P, Wang J, Le Y. Dasatinib nanoemulsion and nanocrystal for enhanced oral drug delivery. *Pharmaceutics.* 2022;14(1):197. doi: 10.3390/pharmaceutics14010197, PMID 35057093.
- Sabra SA, Sheweita SA, Haroun M, Ragab D, Eldemellawy MA, Xia Y. Magnetically guided self-assembled protein micelles for enhanced delivery of dasatinib to human triple-negative breast cancer cells. *J Pharm Sci.* 2019;108(5):1713-25. doi: 10.1016/j.xphs.2018.11.044, PMID 30528944.
- Muthadi RR, Kumar SG. A systematic review on supersaturable self-nano emulsifying drug delivery system: a potential strategy for drugs with poor oral bioavailability. *Int J Appl Pharm.* 2022;14(3):16-33.
- Paranjpe M, Muller Goymann CC. Nanoparticle-mediated pulmonary drug delivery: a review. *Int J Mol Sci.* 2014;15(4):5852-73. doi: 10.3390/ijms15045852, PMID 24717409.
- Babu A, Templeton AK, Munshi A, Ramesh R. Nanoparticle-based drug delivery for therapy of lung cancer: progress and challenges. *J Nanomater.* 2013;2013:1-11. doi: 10.1155/2013/863951.
- Widakowich C, de Castro G, de Azambuja E, Dinh P, Awada A. Review: side effects of approved molecular targeted therapies in solid cancers. *Oncologist.* 2007;12(12):1443-55. doi: 10.1634/theoncologist.12-12-1443, PMID 18165622.
- Byrne JD, Betancourt T, Brannon Peppas L. Active targeting schemes for nanoparticle systems in cancer therapeutics. *Adv Drug Deliv Rev.* 2008;60(15):1615-26. doi: 10.1016/j.addr.2008.08.005, PMID 18840489.
- Yao Q, Choi JH, Dai Z, Wang J, Kim D, Tang X. Improving tumor specificity and anticancer activity of dasatinib by dual-targeted polymeric micelles. *ACS Appl Mater Interfaces.* 2017;9(42):36642-54. doi: 10.1021/acsami.7b12233, PMID 28960955.
- Dong C, Li B, Li Z, Shetty S, Fu J. Dasatinib-loaded albumin nanoparticles possess diminished endothelial cell barrier disruption and retain potent anti-leukemia cell activity. *Oncotarget.* 2016;7(31):49699-709. doi: 10.18632/oncotarget.10435, PMID 27391073.
- Moore TL, Grimes SW, Lewis RL, Alexis F. Multilayered polymer-coated carbon nanotubes to deliver dasatinib. *Mol Pharm.* 2014;11(1):276-82. doi: 10.1021/mp400448w, PMID 24294824.
- Adena SKR, Upadhyay M, Vardhan H, Mishra B. Development, optimization, and *in vitro* characterization of dasatinib-loaded PEG functionalized chitosan capped gold nanoparticles using box-behnken experimental design. *Drug Dev Ind Pharm.* 2018;44(3):493-501. doi: 10.1080/03639045.2017.1402919, PMID 29161920.
- Gossai N, Naumann J, Zamora E, Li NS, Piccirilli J, Gordon PM. Drug-DNA conjugated gold nanoparticles for the treatment of acute myeloid leukemia. *Am Soc Hematol.* 2015;126(23):4935.
- Wei L, Sun P, Nie S, Pan W. Preparation and evaluation of SEDDS and SMEDDS containing carvedilol. *Drug Dev Ind Pharm.* 2005;31(8):785-94. doi: 10.1080/03639040500216428, PMID 16221613.

17. Prajwal N, Aparna J, Dipti S, Shubhangi A. Revolutionizing pharmaceuticals: a deep dive into self-nanoemulsifying drug delivery systems. *Int J Curr Pharm Res.* 2024;16(1):1-9.
18. Kasturi M, Agrawal S, Janga KY. Self nano emulsifying drug delivery system of ramipril: formulation and *in vitro* evaluation. *Int J Pharm Pharm Sci.* 2016;8(4):291-6.
19. Singh G, Pai RS. Trans-resveratrol self-nano-emulsifying drug delivery system (SNEDDS) with enhanced bioavailability potential: optimization, pharmacokinetics and *in situ* single pass intestinal perfusion (SPIP) studies. *Drug Deliv.* 2015;22(4):522-30. doi: 10.3109/10717544.2014.885616, PMID 24512464.
20. Brouwers J, Brewster ME, Augustijns P. Supersaturating drug delivery systems: the answer to solubility-limited oral bioavailability? *J Pharm Sci.* 2009;98(8):2549-72. doi: 10.1002/jps.21650, PMID 19373886.
21. Jeevana JB, Sowmya M. Design of gastroretentive polymeric low-density microballoons of mebendazole using response surface methodology. *Asian J Pharm Clin Res.* 2022;15(7):149-59.
22. Hema AN, Gaayathri G, Gundeti S. Development of orodispersible tablets of loratadine containing an amorphous solid dispersion of the drug in soluplus® using design of experiments. *Int J Pharm Pharm Sci.* 2023;15(8):19-27.
23. Oyejola BA, Nwanya JC. Selecting the right central composite design. *Int J Stat Appl.* 2015;5(1):21-30.
24. Quinlan PJ, Tanvir A, Tam KC. Application of the central composite design to study the flocculation of an anionic azo dye using quaternized cellulose nanofibrils. *Carbohydr Polym.* 2015;133:80-9. doi: 10.1016/j.carbpol.2015.06.095, PMID 26344258.
25. Wang L, Dong J, Chen J, Eastoe J, Li X. Design and optimization of a new self-nanoemulsifying drug delivery system. *J Colloid Interface Sci.* 2009;330(2):443-8. doi: 10.1016/j.jcis.2008.10.077, PMID 19038395.
26. Date AA, Nagarsenker MS. Design and evaluation of self-nanoemulsifying drug delivery systems (SNEDDS) for cefpodoxime proxetil. *Int J Pharm.* 2007;329(1-2):166-72. doi: 10.1016/j.ijpharm.2006.08.038, PMID 17010543.
27. Shivakumar HN, Patel PB, Desai BG, Ashok P, Arulmozhi S. Design and statistical optimization of glipizide loaded lipospheres using response surface methodology. *Acta Pharm.* 2007;57(3):269-85. doi: 10.2478/v10007-007-0022-8, PMID 17878108.
28. Mahmoud H. Design and optimization of self-nanoemulsifying drug delivery systems of simvastatin aiming dissolution enhancement. *Afr J Pharm Pharmacol.* 2013;7(22):1482-500. doi: 10.5897/AJPP2013.2987.
29. Kallakunta VR, Bandari S, Jukanti R, Veerareddy PR. Oral self emulsifying powder of lercanidipine hydrochloride: formulation and evaluation. *Powder Technol.* 2012;221:375-82. doi: 10.1016/j.powtec.2012.01.032.
30. Tran TH, Guo Y, Song D, Bruno RS, Lu X. Quercetin-containing self-nanoemulsifying drug delivery system for improving oral bioavailability. *J Pharm Sci.* 2014;103(3):840-52. doi: 10.1002/jps.23858, PMID 24464737.
31. Zhang P, Liu Y, Feng N, Xu J. Preparation and evaluation of self-microemulsifying drug delivery system of oridonin. *Int J Pharm.* 2008;355(1-2):269-76. doi: 10.1016/j.ijpharm.2007.12.026, PMID 18242895.
32. Kollipara S, Gandhi RK. Pharmacokinetic aspects and *in vitro-in vivo* correlation potential for lipid-based formulations. *Acta Pharm Sin B.* 2014;4(5):333-49. doi: 10.1016/j.apsb.2014.09.001, PMID 26579403.
33. Yoo J, Baskaran R, Yoo BK. Self-nanoemulsifying drug delivery system of lutein: physicochemical properties and effect on bioavailability of warfarin. *Biomolecules and Therapeutics.* 2013;21(2):173-9. doi: 10.4062/biomolther.2013.011.
34. Yadav P, Rastogi V, Verma A. Application of box-behnken design and desirability function in the development and optimization of self-nanoemulsifying drug delivery system for enhanced dissolution of ezetimibe. *Futur J Pharm Sci.* 2020;6(1):7. doi: 10.1186/s43094-020-00023-3.
35. Dash RN, Mohammed H, Humaira T, Reddy AV. Solid supersaturatable self-nanoemulsifying drug delivery systems for improved dissolution, absorption and pharmacodynamic effects of glipizide. *J Drug Deliv Sci Technol.* 2015;28:28-36. doi: 10.1016/j.jddst.2015.05.004.